Multielectron excitations in the L-subshell photoabsorption of xenon

Iztok Arčon, Alojz Kodre, Matjaž Štuhec, and Denis Glavič-Cindro
Jožef Stefan Institute, Jamova 39, 61111, Ljubljana, Slovenia
and Department of Physics, University of Ljubljana, Slovenia

Wolfgang Drube
Hamburger Synchrotronstrahlungslabor at Deutsches Elektronen Synchrotron DESY, Hamburg, Germany
(Received 24 May 1994)

Multielectron excitations in x-ray absorption of xenon in the energy region of the L edges are studied. Broad structures in the subshell absorption spectra are attributed to virtual collective excitations such as core relaxation and dielectric polarization. Three groups of sharp spectral features, corresponding to multielectron transitions involving $5p$, $5s$, and $4d$ electrons, respectively, are found. Due to the large lifetime width and multiplet spread, the features are superpositions of individual transitions within a group. From comparison of corresponding features in the three L-subshell spectra, some conclusions on the role of the inner-shell vacancy in the process can be drawn. Differences in L_1 and $L_{2,3}$ spectral features generally point to a complex excitation mechanism, although some cases seem to obey the simple sudden approximation. Evidence for a strongly coupled outer-shell excitation involving the $4d$ subshell is found.

PACS number(s): 32.30.Rj, 32.80.Fb

I. INTRODUCTION

The possibility of multielectron excitation in the atomic inner-shell photoeffect was first demonstrated by measurements of fluorescence [1] and Auger satellites [2]. In its high-energy limit the phenomenon was satisfactorily explained by the sudden change of the effective potential [3–5]. In the near-threshold regime, a more complex explanation including a contribution of the electron correlations [6] is required, providing a sensitive test of theoretical models. X-ray absorption spectrometry, the predominant experimental tool [7–21], has provided evidence of the process in a number of atomic systems. The onset of multielectron excitation or ionization channels is revealed by sharp features in the energy dependence of the photoabsorption cross section. Due to the low probability of the multielectron channels relative to the single-electron photoeffect, these features can only be resolved clearly in conditions of free-atom absorption, i.e., in experiments on noble gases and metallic vapors [22,23]. In compound and solid absorbers, the multielectron features are masked by the molecular or condensed-phase effects in the x-ray absorption [24–29].

Usually, the multielectron components in absorption spectra are first identified by their energies: a sharp spectral feature appearing close to the calculated energy of a multiply excited atomic state is used as evidence for a particular reaction channel. However, it has become recognized that the spectra cannot always be decomposed merely into small additional resonances, absorption edges, and changes of slope, corresponding to thresholds of transitions to consecutive higher excited states and singly or doubly ionized states, respectively. More complex spectral features, arising from the interaction of channels, as well as from the configuration interaction in both final and initial states, are often found. They can only be unraveled by a calculation of transition probabilities: the complete reconstruction of the measured cross section represents a much more stringent test of the theory and has been successfully carried out only for a few cases [21,30–33].

In all reliable absorption experiments on multielectron photoexcitation, the formation of an inner-shell vacancy has only been observed to induce excitations in the two outermost shells. Of these, the outer-shell excitations in noble gases contribute a rich, detailed spectrum, while the excitations in the second outermost shell, as a rule, show little detail, hardly resolvable in state-of-the-art experiments. Besides this overall similarity, the best-studied cases are too far apart and too dissimilar that much general insight could be gained by comparing them, even after a successful theoretical reconstruction. The spectra are governed by different details of the level scheme and lifetime widths. To overcome this obstacle, several attempts at investigations on closely related systems have recently been reported [27,29]. One of the simplest possibilities is the absorption spectrometry at different absorption edges of the same atom. From such collection of spectra, the effect of direct correlation could be recognized from differences in related multielectron features: excitations of outer electrons, caused by the change of the average potential, on the other side, should be largely independent of the inner-shell vacancy. L-subshell spectra are most promising in this respect due to the comparable lifetime widths of the inner-shell vacancy states.

We have devised such an experiment on xenon. The atom has been extensively used as a test for theoretical models, due to the strong orbital rearrangement in the Xe–Ba series. The photoabsorption spectrum above the K edge of xenon shows almost no detail due to the large K-shell width (11.4 eV) [18], providing only little information about its multiple excitations. The published re-

sults on the L-shell multielectron excitations [34], although incomplete in subshell data, indicate interesting similarities as well as dissimilarities, so that a systematic remeasurement seems warranted.

II. EXPERIMENT

The experiment was performed at the EXAFS II station at Hamburger Synchrotronstrahlungslabor. The synchrotron radiation from the DORIS storage ring running at 5.3 GeV and 40 mA was focused by a gold-coated mirror on a Si(111) double-crystal monochromator with 1-eV resolution at 5 keV. Harmonics were effectively eliminated by detuning the monochromator crystals using a stabilization feedback control.

The xenon gas sample, of purity 99.995%, was contained in a 40-mm-long absorption cell with 0.5-mm Lucite windows, at the pressure of 12.0 kPa at 24 °C, providing the absorption thickness of the gas close to the optimum $\mu d \approx 2$. The absorption cell was inserted in the vacuum path of the monochromatized beam between two nitrogen-filled ionization chambers monitoring the intensities of the incident and the transmitted beam, I_0 and I_t, respectively. The energy region of the xenon L edges was scanned in steps of 0.2 eV. The integration time at each step of the scan was 1 s and the incident photon flux was 10^{10} photons/s.

The absorption cell can be evacuated and refilled independently without changing its position in the beam. In this way, high reproducibility of the scans is achieved: for every absorption spectrum, a corresponding reference spectrum without the absorbing gas in the cell can be taken in identical conditions. By subtracting the reference attenuation $\ln(I_0/I_t)$ from the respective attenuation of the xenon-filled cell, the sensitivities of the ionization chambers and the residual absorption of the cell windows cancel out and the absolute value of the absorption thickness μd of the sample gas is obtained.

III. DATA EVALUATION

The measured attenuation cross section of xenon in the energy region of the L edges is shown in Fig. 1. The accuracy of the absolute scale is limited to 2% by the uncertainty of the manometer reading: the scatter of the experimental points, due mainly to the synchrotron beam noise, is 15 b. The precise energy scale is established using experimental Xe L-level energies [35]. The comparison of the measured spectrum and the theoretical frozen-core one-electron photoabsorption cross section given by Scofield [36] shows good agreement below the L_3 edge and far above the L_1 edge, as expected from the theoretical argument by Fadley [37] that the frozen-core one-electron cross sections correspond to the total rather than the single-electron ionization cross section in the sudden-approximation high-energy limit. Sharp spikes at the L_2 and L_3 edges are the absorption white lines due to $2p \rightarrow nd$ transitions, not included in Scofield's calculation. The white line at the L_1 edge, as shown by Breinig *et al.* [35], does not produce a spike. To enhance the comparison, both sets of data are divided by a simple power-law (E^{-a}) interpolation of cross sections from the independent-particle model by Sasaki [38] (Fig. 2).

Large-scale deviations from Scofield's predictions in the entire interedge region can be attributed to two distinct effects which have been observed and studied on other atomic systems. Immediately above the L_1 edge, the measured cross section exhibits a steeper slope which levels out within 70 eV. The width of the region is too large to be attributed to the formation of an excited state.

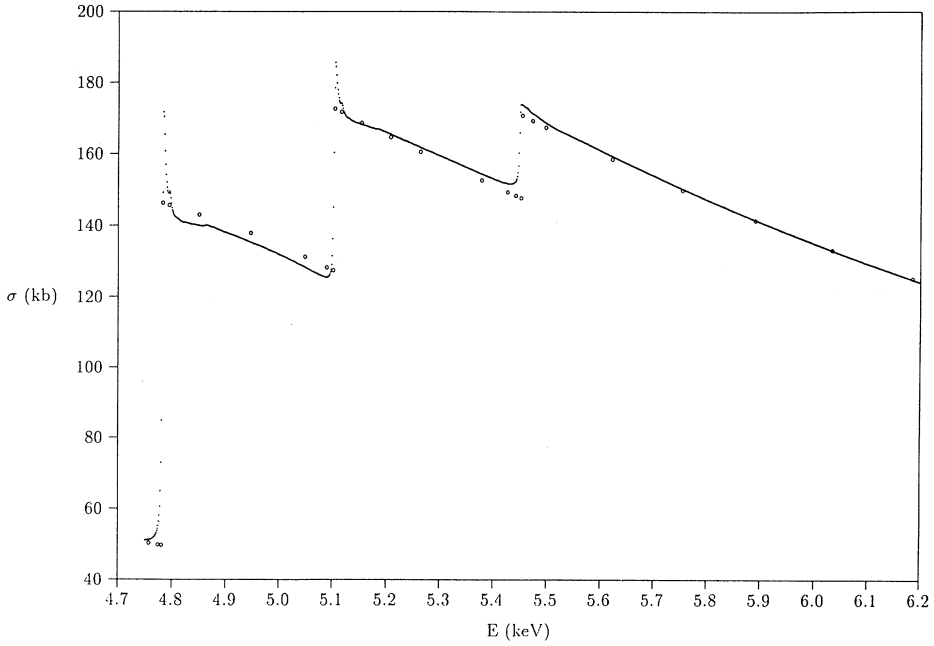

FIG. 1. Attenuation cross section of xenon in the energy region of the L edges. . . ., experiment; ooo, theoretical frozen-core one-electron photoabsorption cross section given by Scofield [36].

According to Tulkki and Åberg [39,40], in the slow process of photoionization immediately above the edge, the cross section is enhanced by core relaxation and by the additional reorganization in the Auger decay of the vacancy with the slow photoelectron still within the atom (post-collision interaction [41]). The effect has been observed at the K edges of argon [39], krypton [12], and xenon [17]. In the case of the L_2 and L_3 edges the effect is masked by the white lines: after their contribution is removed, smaller regions of steeper slope extending to ≈ 20 eV above the edge are revealed.

Between the edges, the cross section in Fig. 1 exhibits a slightly convex curvature instead of the usual concave one. Similar deviations have been studied in the L absorption spectra of heavy elements from Hf to Pb [42]. They are attributed to the dielectric polarization of the $2p$ subshells, which introduces dispersionlike dips at the L_2 and L_3 edges, hence the change of the curvature, and also the difference in slopes of measured and Scofield's data in the L_2 region, seen in Fig. 2.

In contrast to these large and extended effects, the spectral features introduced by the multielectron excitations are small and sharp, consisting of tiny resonance peaks and absorption edges, characterized by the lifetime width ≈ 3 eV of L vacancy states. They only become apparent after the suppression of the dynamic range of the experimental data, i.e., after subtraction of the large-scale effects, discussed above. In the absence of satisfactory theoretical predictions, a best-fit analytical model, a combination of a second-order polynomial and an exponen-

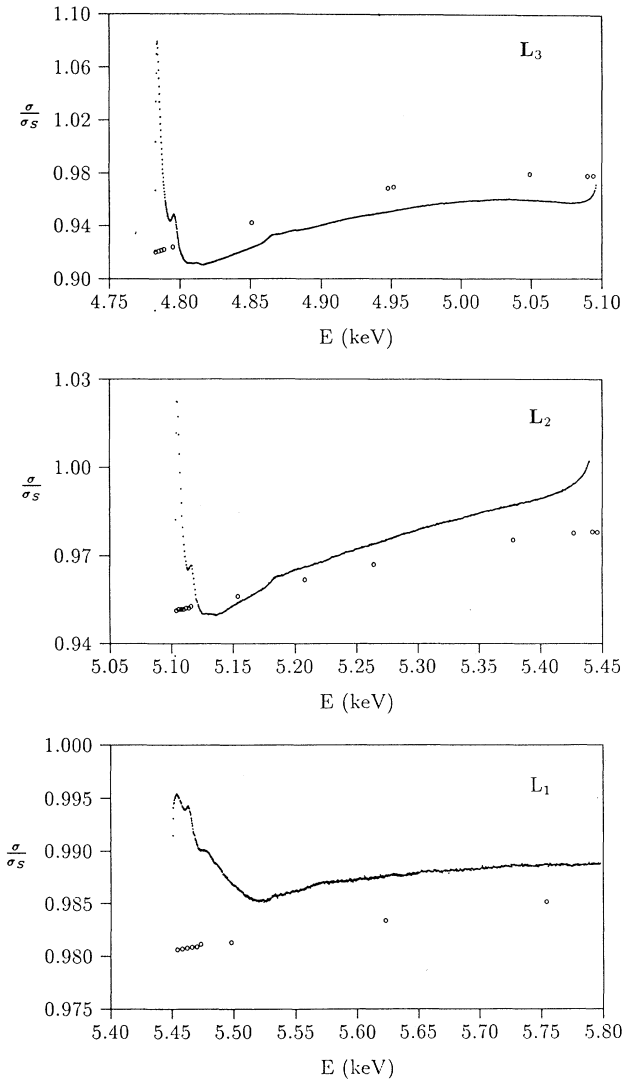

FIG. 2. Deviation of the measured photoabsorption cross section from Scofield's theoretical predictions. Both sets of data are divided by a power-law interpolation of the independent-particle cross section (σ_S) [38].

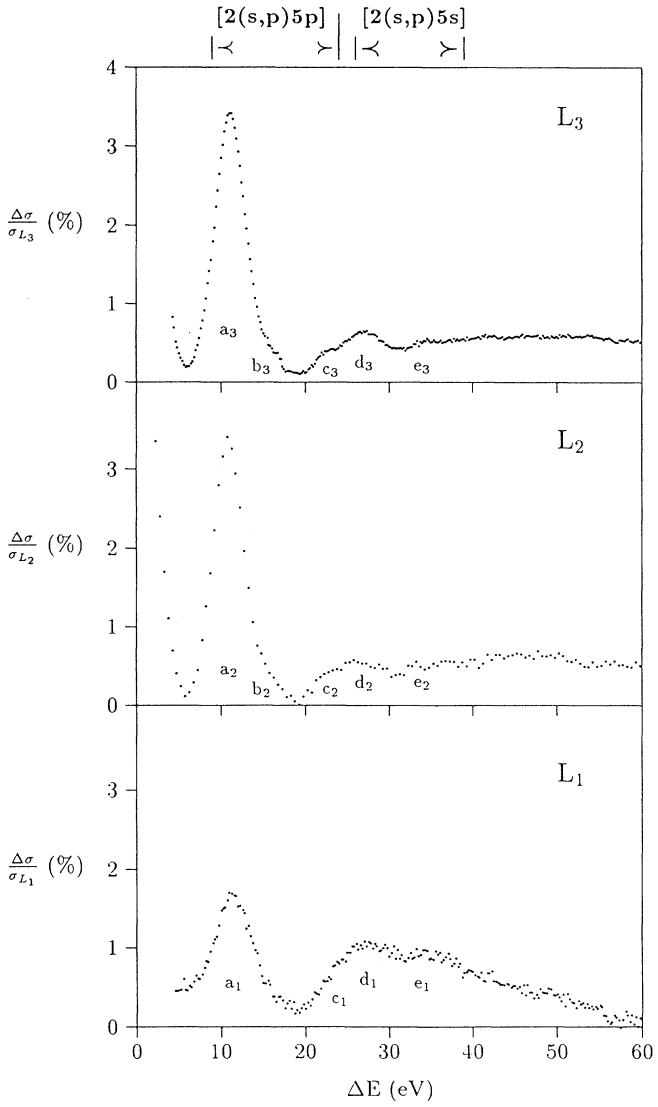

FIG. 3. Multielectron photoabsorption features of xenon in the L edge region. Cross sections are normalized to the respective L-subshell edge jumps. The common energy scale is defined relative to the respective L-subshell edge. MCDF energy intervals, belonging to the additional excitations of electrons from $5p$ and $5s$ subshells, respectively, are shown.

tial, is used. In the procedure, several groups of multielectron absorption features are revealed (Figs. 3 and 4) in each subshell spectrum.

It should be stressed at this point that the use of *ad hoc* models, however unavoidable and common practice, obscures the long-range nature of the small absorption features. Only the abrupt elements of the features, such as peaks and jumps, can be reliably recognized, while the asymptotic increase of the cross section due to the shake-up and shake-off contributions cannot be resolved in the best-fit procedure.

IV. MULTIELECTRON EXCITATIONS

The procedure described above reveals a fine-scale absorption structure extending to 200 eV above each of the L subshell edges. For the purpose of comparison, the three spectra shown in Figs. 3 and 4 are brought to the common relative energy scale with the origin at each respective L-subshell edge. Similarly, cross sections are normalized to the respective L-subshell edge jumps, extrapolated from Scofield's data. Several individual features can be recognized within the structures: they appear at the same positions on the relative energy scale in all three subshell spectra. Accordingly, they will be referred to by common labels $(a-i)$ and distinguished by L-subshell indices (Table I). Even without detailed analysis, it is evident that the corresponding features, and indeed the whole structure, above the L_2 and L_3 edges are identical within the accuracy of the experiment, while those of the L_1 spectrum differ from their counterparts in size and width; some may even be missing.

For the purpose of interpretation of the measured spectra, an extensive survey of multiconfiguration Dirac-Fock (MCDF) energies of L-vacancy xenon states with additional excitation in the outer shell has been made [43]. Notably, the energies of the states with the same outer-shell vacancy configuration and different L-subshell vacancy were found to agree to better than 1 eV on the relative scale, introduced above. This is in accord with the coincidence of the labeled features in the three L-subshell spectra.

By their energies, these MCDF states can be divided into three nonoverlapping groups with additional excitations of electrons from $5p$, $5s$, and $4d$ subshells, respectively. The corresponding energy intervals are shown in Figs. 3 and 4. They are bracketed by the lowest double excitation on the low-energy side and by the double ionization (shake-off) on the high-energy side. In the case of the $5p$, group in the L_1 spectrum, for instance, the brackets are set at the lowermost energy in the multiplet $Xe[2s5p]6p^2$ and the highermost energy in the multiplet $Xe[2s5p]$, respectively.

In contrast to the well-known multielectron absorption structures above the K edges of argon [9,19] and krypton [10], the spectral features in the present case cannot be identified with transitions to individual doubly excited states. The reason is of a fundamental nature: the multiplet splitting of the double-vacancy states is much larger

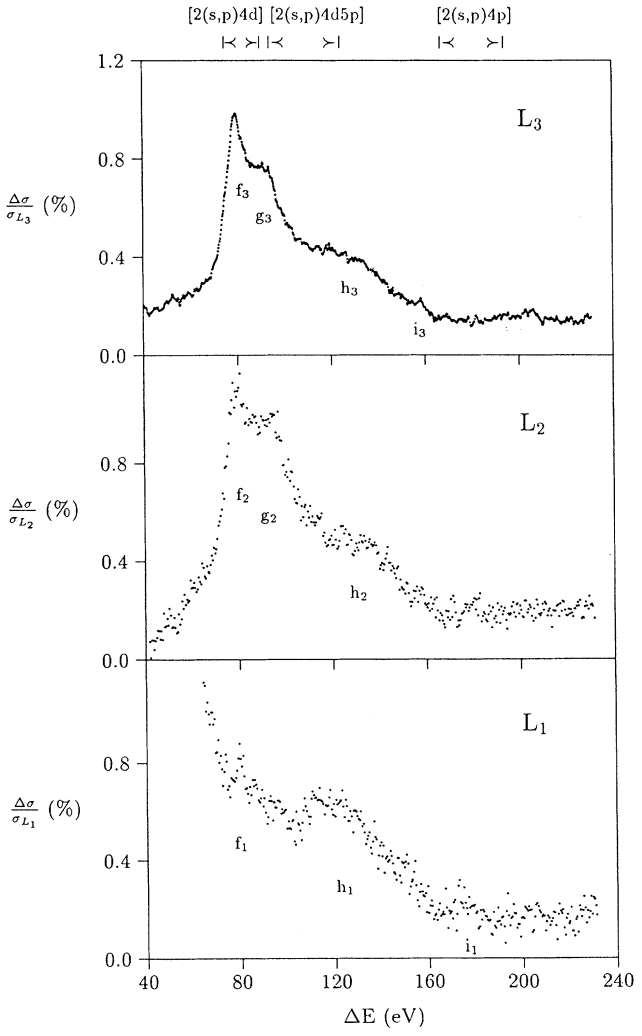

FIG. 4. Same as Fig. 3 but for the $4d$ excitation group.

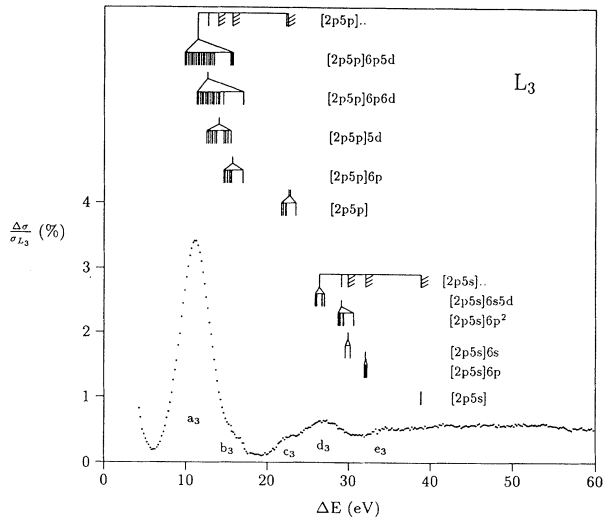

FIG. 5. Conventional level scheme for the case of the $[2p5(p,s)]$ group of multielectron excitations in Xe.

TABLE I. Parameters of multiple-excitation spectral features $a-i$ above xenon L edges, according to tentative type (R, resonance; E, absorption edge; RR, broad resonance): energy, relative to the respective L-subshell edge; width; and cross section, relative to the respective L-subshell jump. Features are grouped according to the outer-electron state.

		L_3			L_2			L_1			
Label	Type	E (eV)	Γ (eV)	σ_F/σ_{L_3} (%)	E (eV)	Γ (eV)	σ_F/σ_{L_2} (%)	E (eV)	Γ (eV)	σ_F/σ_{L_1} (%)	Group
a	R	11.2±0.5	4.2±0.1	3.0±0.2	10.9±0.5	4.2±0.1	3.3±0.2	11.5±0.5	4.5±0.2	1.3±0.3	
b	R	15.7±0.5	3.0±0.5	0.3±0.05	15.6±0.7	3.0±0.5	0.3±0.05				[5p]
c	E	21.3±0.5	2.0±1.0	0.4±0.1	20.9±0.7	2.4±1.0	0.6±0.3	21.5±0.5	2.2±0.7	0.9±0.3	
d	R	27.0±0.5	4.0±1.0	0.2±0.05	26.8±0.8	5.0±1.0	0.2±0.1	26.9±0.7	4.0±1.0	0.2±0.1	[5s]
e	E	33.1±0.05	2.0±1.0	0.1±0.05	32.3±1.0	2.0±1.0	0.1±0.05	33.6±1.0	2.3±1.0	0.14±0.07	
f	R	80.0±0.5	7.4±0.5	0.5±0.05	78.7±0.5	7.6±0.5	0.4±0.06	79.6±0.6	7.0±1.0	0.2±0.1	[4d]
g	BR	91.1±0.7	26.1±0.5	0.6±0.1	89.6±1.5	29.4±3.0	0.8±0.1				
h	BR	128.4±1.0	36.7±2.0	0.3±0.05	127.2±2.0	37.6±4.0	0.3±0.05	128.3±1.0	37.8±2.0	0.4±0.1	[4d5p]

than in the case of Ar and Kr, so that multiplets of accessible excitations within a group strongly overlap. As an example, the conventional level scheme is shown in Fig. 5 for the case of the [$2p5(p,s)$] group. Evidently, the spectral features must be interpreted as superpositions of a number of individual resonances and absorption edges. Only the leading resonance of each group is, rather tentatively, attributed to the transition into the lowermost excited state (Table II): this has been, as a rule, the case with the strongest resonances in the spectra of previously studied atoms.

For the same reason as above, there is little need to expand the search for candidate states beyond the double excitations, although good evidence has been given for triple-vacancy states in the spectra of argon [44] and krypton [20]. In the present case, their contribution to the spectral features would be smeared out beyond recognition for the correspondingly larger spread of their multiplet structure. Triply excited states will, though, be invoked for reasons of analogy, for features that extend beyond double-excitation energy brackets.

A. [$2(s,p)5(p,s)$] excitations

Although the groups of $5p$ and $5s$ MCDF excitation energies are clearly separated, the spectral features attributed to both groups overlap. The detailed level scheme, given in Fig. 5, shows that the multiplet spread is indeed the determining factor in the case of Xe spectra. The multiplets of doubly excited states reach beyond the ionization limits: this leads to resonance-continuum interaction and introduces Fano profiles into spectral features. Consequently, there is little hope to identify the labeled features, apart from the leading resonances of each group, with distinct excitations. The pronounced valley between the two groups, suggestive of a small absorption edge (c) on its high-energy side, cannot be brought into accord with the level scheme.

The effect of configuration mixing in the final state was analyzed. Significant mixing was found only between the states [$2s5p$]$6p^2,5d^2$, analogous to the case of argon: [$1s3p$]$4p^2,3d^2$ [31,32]. The widths of the observed resonances are again in accord with the energy splitting of the multiplets of the corresponding final states. Thus the adoption of mixing does not substantially clarify the shape of the measured spectrum: the interpretation will have to wait until a complete theoretical reconstruction of the cross section is made.

B. [$2(s,p)4d$] excitations

The sharp resonances f at the onset of the $4d$ group can be reliably attributed to the [$2s4d$]$6p5d$ and

TABLE II. Most probable transitions contributing to the observed resonances. Energy intervals of MCDF multiplets are compared to the positions and the widths of the resonances.

	Configuration	E^{MCDF} (ev)	Feature	E^{expt} (eV)	Γ^{expt} (eV)
$L_{2,3}$	[$2p5p$]$6p5d$	9.8–13.4	$a_{2,3}$	11.2±0.5	4.2±0.1
		15.4–15.8	$b_{2,3}$	15.7±0.5	3.0±0.5
	[$2p5s$]$6s5d$	25.9–27.2	$d_{2,3}$	27.0±0.5	4.0±1.0
	[$2p4d$]$5d^2$	75.8–81.4	$f_{2,3}$	80.0±0.5	7.4±0.5
L_1	[$2s5p$]$6p^2,5d^2$	10.5–16.2	a_1	11.5±0.5	4.5±0.2
	[$2s5s$]$6s5p$	26.3–28.7	d_1	26.9±0.7	4.0±1.0
	[$2s4d$]$6p5d$	76.8–82.0	f_1	79.6±0.5	7.0±1.0

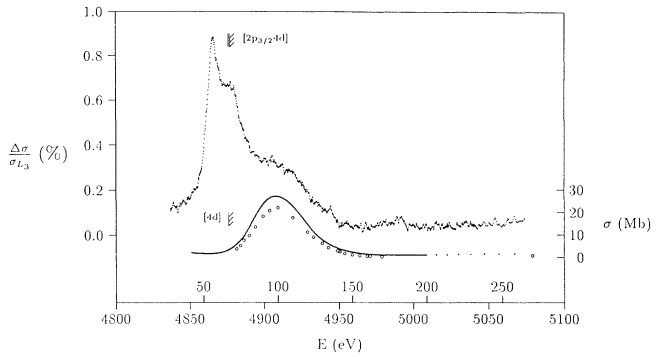

FIG. 6. Photoabsorption cross section of xenon in the energy region of $[2p_{3/2}4d]$ excitations, compared to the total vuv photoabsorption cross section (——) and the $4d$ partial cross section (ooo) of Xe in the energy region of the $4d$ edge [46]. The $4d$ ionization threshold is shifted to coincide with the $[2p_{3/2}4d]$ double-ionization threshold in the L_3-subshell spectrum.

$[2p4d]5d^2$ excitations. In view of the multiplicity of the $4d$ states, the small width is rather surprising: in fact, the analogous double excitations involving the $3d$ shell in Kr produce an extremely broad spectral feature [13,20]. The shoulders g, absent in the L_1 spectrum, cannot be identified unambiguously: a comparison with the MCDF energies points to a superposition of excitations to higher states and to the continuum, including possible triple excitations [. . .$4d5p$].

The broad peaks h, remarkably similar in all three subshell spectra, lie well outside the recognized MCDF energy brackets. Their width and position in the relative energy scale bring them into correspondence with the "shape resonance" in the vacuum ultraviolet (vuv) photoabsorption spectra above the $4d$ absorption edge of xenon and its neighboring elements [45,46]. A direct comparison is shown in Fig. 6. Apparently, the strong influence of the effective atomic potential on the final-state continuum wave function εf, resulting in the shape resonance in the $4d \rightarrow \varepsilon f$ excitations [45], is retained in the cross section for the indirect excitations of $4d$ subshells. Amusia *et al.* have given arguments that the shape resonance has a strong double-excitation component, arising from the inelastic scattering of the $4d$ photoelectron by electrons in the outermost $5p$ shell [47]. By analogy, triple excitations $[2(p,s)4d5p]$ can be expected to contribute significantly to the structures h.

C. $[2(p,s)4(p,s)]$ and $[2(p,s)3d]$ excitations

An extensive search in the energy region where accompanying excitations of $4p$, $4s$, and $3d$ electrons can be expected revealed no features that could be reliably identified. Estimated from the sensitivity of the experiments, the cross sections for these excitations should be below 30 b. A possible exception are two peaks, in the L_1 and L_3 spectra, labeled i and seen above the noise level only in the best of experimental conditions, attributed to resonant excitations of $[2s4p]$ and $[2p_{3/2}4p]$ vacancy states. The finding is supported by a subsequent investigation of Xe-like ions where cross sections for multiple excitations are found to increase substantially with atomic number [48]. The $4p$ resonances in La^{3+} are clearly resolved.

According to the results of Wendin and Ohno [49] on the direct $4p$ photoeffect, in Xe and preceding elements the dipolar fluctuations of the $4p$ vacancy prevent the existence of $[4p]$ as a quasistationary state, forcing it to dissociate very rapidly into more complicated states, where the dominant process yields the $4d^84f$ configuration. However, in subsequent elements, a well-defined $4p_{3/2}$ quasihole exists as a stable excitation with its MCDF binding energy lowered by about 10 eV due to the many-electron interactions, while the $[4p_{1/2}]$ state is still dissociated into a broad range of $4d^84f$ configurations. Since for outer electrons the atomic potential in a xenon atom with a vacancy in the L shell is approximately the same as in neutral cesium, the sharp i structures should specifically be attributed to the discrete transitions to $[2p_{3/2}4p_{3/2}]$ or $[2s4p_{3/2}]$ final states.

V. DISCUSSION

The measured spectra give information regarding the role of the inner-shell vacancy in multiple photoexcitation: a p-type vacancy is studied systematically and a direct comparison of the effect of s- and p-type vacancies, close in energy, is given. One conclusion is rather self-evident: the identical L_2 and L_3 spectra show that multiple photoexcitation is largely independent of the spin of the inner-shell vacancy or its total angular momentum. Possible differences, arising from different multiplet structure of $[2p_{1/2}]$ and $[2p_{3/2}]$ states or from different shapes of their relativistic wave function, are below the present sensitivity of the experiment.

The marked difference between L_1 and $L_{2,3}$ spectra, on the other hand, provides some insight into the mechanism of double excitations. Considering the large spatial and energy separation of both excited electrons, it could be expected that their direct interaction has a much weaker effect than the shake mechanism, i.e., the excitation of the outer shells by the sudden change in the core charge. In the latter case, it would be possible, to a good approximation, to factor the probability for the multiple excitations into two parts: the probability for the photoeffect in the core and the probability for additional excitation of outer electrons. Since the relative energies and widths of multiply excited states are almost independent of the core-vacancy subshell, the normalized L-subshell multielectron absorption spectra should be largely identical.

Our experimental results indicate that this simple explanation is insufficient. The detailed evidence is provided by the data shown in Table I in the form of relative cross sections attributed to individual spectral features. Regardless of the low accuracy of extracted values, there appears to be a regularity in the ratio of L_1-to $L_{2,3}$ data. The values for the features d, e, and h are close to 1, supporting the dominance of the shake picture. However, for the best-resolved resonant features a and f, the ratio of probabilities is near 0.5, and for the feature c, over 2.

Thus it seems necessary to generally invoke complex mechanisms even at the present crude level of identification of the spectra, although they may simplify to the shake picture for some channels.

(It might seem, with the factorization picture in mind, that the cross sections for the resonant, double excitation channels are not properly normalized to the subshell edge jump which involves the matrix element between the core and the continuum. A better choice for the normalization would seem to be the cross section of the single-electron excitation, the "white-line" transition. However, in the case of Xe L subshells, as has been demonstrated by Breinig *et al.* [35], discrete pre-edge transitions are of the same relative site to the edge jump for all three subshells.)

The simple shake picture holds surprisingly well for the excitations involving $4d$ subshells, contributing to the broad resonances h. The reason for such a behavior may be that the shape of the final f states is determined by the potential barrier so that the cross section is independent of the primary excitation. The remarkable fact that absorption features of similar shape and comparable width are found in direct photoexcitation, as well as in the indirect excitation accompanying core-electron photoeffect in three different subshells, indicates the existence of a strongly coupled outer-shell excitation.

VI. CONCLUSION

Summarily, the deviations of the measured photoabsorption cross section above L edges of Xe from the smooth single-electron model are of two distinct types. The long-range effects can be attributed to virtual collective excitations of the electron clouds such as core relaxation and the dielectric polarization. They have been observed in other atomic systems. Sharp absorption features, presumably superpositions of resonances and absorption edges, correspond to real multiple excitations. Again, as in all cases to date, only excitations in the two outermost shells are reliably determined. The large lifetime width and the multiplet spread do not allow clear identification of the features beyond the assignation to the $5p$ $5s$, or $4d$ subshell group. However, it is shown that new information can be extracted from a comparison of closely related multiple-excitation spectra. In extension of the present work, the study of Xe-like ions is under way.

ACKNOWLEDGMENTS

The work was supported by Ministry of Science and Technology of Slovenia and Internationales Buro Juelich. Professor U. Becker kindly provided original VUV data in Fig. 6.

[1] R. D. Deslattes, Phys. Rev. **133**, A390 (1964); **133**, A399 (1964).
[2] M. O. Krause, T. A. Carlson, and R. D. Dismukes, Phys. Rev. **170**, 37 (1968).
[3] T. Åberg, Phys. Rev. **156**, 35 (1967).
[4] T. A. Carlson, C. W. Nestor, T. C. Tucker, and F. B. Malik, Phys. Rev. **169**, 27 (1968).
[5] T. A. Carlson and C. W. Nestor, Phys. Rev. A **8**, 2887 (1973).
[6] R. L. Martin and D. A. Shirley, J. Chem. Phys. **64**, 3685 (1976).
[7] H. W. Schnopper, Phys. Rev. **131**, 2558 (1963).
[8] F. Wuilleumier, J. Phys. (Paris) **26**, 776 (1965).
[9] R. D. Deslattes, R. E. LaVilla, P. L. Cowan, and A. Henins, Phys. Rev. A **27**, 923 (1983).
[10] M. Deutsch and M. Hart, Phys. Rev. Lett. **57**, 1566 (1986).
[11] M. Deutsch and M. Hart, Phys. Rev. A **34**, 5168 (1986).
[12] M. Deutsch and M. Hart, J. Phys. B **19**, L303 (1986).
[13] E. Bernieri and E. Burattini, Phys. Rev. A **35**, 3322 (1987).
[14] S. Bodeur, P. Millie, E. Lizon a Lugrin, I. Nenner, A. Filipponi, F. Boscherini, and S. Mobilio, Phys. Rev. A **39**, 5075 (1989).
[15] A. Kodre, S. J. Schaphorst, and B. Crasemann, in *X-Ray and Inner-Shell Processes,* Proceedings of the Fifteenth International Conference on X-Ray and Inner-Shell Processes, Knoxville, 1990, AIP Conf. Proc. No. 215, edited by T. A. Carlson, M. O. Krause, and S. T. Manson (AIP, New York, 1990), p. 582.
[16] U. Kuetgens and J. Hormes, Phys. Rev. A **44**, 264 (1991).
[17] M. Deutsch, G. Brill, and P. Kizler, Phys. Rev. A **43**, 2591 (1991).
[18] M. Deutsch and P. Kizler, Phys. Rev. A **45**, 2112 (1992).
[19] M. Deutsch, N. Maskil, and W. Drube, Phys. Rev. A **46**, 3963 (1992).
[20] Y. Ito, H. Nakamatsu, T. Mukoyama, K. Omote, S. Yoshikado, M. Takahashi, and S. Emura, Phys. Rev. A **46**, 6083 (1992).
[21] J. Schaphorst, A. Kodre, J. Ruscheinski, B. Crasemann, T. Åberg, J. Tulkki, M. H. Chen, Y. Azuma, and G. S. Brown, Phys. Rev. A **47**, 1953 (1993).
[22] A. Filipponi, L. Otaviano, and T. A. Tyson, Phys. Rev. A **48**, 2098 (1993).
[23] J. M. Esteva, A. ElAfif, C. Teodorescu, R. C. Karnatak, and M. Womes, J. Phys. (Paris) Colloq. (to be published).
[24] R. Frahm, W. Drube, I. Arčon, D. Glavic-Cindro, M. Hribar, and A. Kodre, in Proceedings of the Second European Conference on Progress in X-Ray Synchrotron Radiation Research, Rome, 1989, edited by A. Balerna, E. Bernieri and S. Mobilio (SIF, Bologna, 1990), Vol. 25, p. 129.
[25] J. Chaboy, J. Garcia, A. Marcelli, and M. F. Ruiz-Lopez, Chem. Phys. Lett. **174**, 389 (1990).
[26] A. Kodre, M. Hribar, I. Arčon, D. Glavič-Cindro, M. Štuhec, R. Frahm, and W. Drube, Phys. Rev. A **45**, 4682 (1992).
[27] G. Li, F. Bridges, and G. S. Brown, Phys. Rev. Lett. **68**, 1609 (1992).
[28] M. Takahashi, S. Emura, K. Omote, S. Yoshikado, Y. Ito, N. Takahashi, and T. Mukoyama, Bull. Inst. Chem. Res. Kyoto Univ. **71**, 37 (1993).
[29] A. Filipponi, T. A. Tyson, K. O. Hodgson, and S. Mobilio, Phys. Rev. A **48**,1328 (1993).
[30] V. L. Sukhorukov, A. N. Hopersky, I. D. Petrov, V. A. Yavna, and V. F. Demekhin, J. Phys. (Paris) **48**, 1677 (1987).

[31] J. W. Cooper, Phys. Rev. A **38**, 3417 (1988).
[32] H. P. Saha, Phys. Rev. A **42**, 6507 (1990).
[33] V. L. Sukhorukov, A. N. Hopersky, and I. D. Petrov, J. Phys. II (Paris) **1**, 501 (1991).
[34] K. Zhang, E. A. Stern, J. J. Rehr, and F. Ellis, Phys. Rev. B **44**, 2030 (1991).
[35] M. Breinig, M. H. Chen, G. E. Ice, F. Parente, and B. Crasemann, Phys. Rev. A **22**, 520 (1980).
[36] J. H. Scofield (unpublished).
[37] C. S. Fadley, Phys. Rev. Lett. **25**, 225 (1974).
[38] S. Sasaki, National Laboratory for High Energy Physics Japan, Report No. KEK 83-22, 1984 (unpublished).
[39] J. Tulkki and T. Åberg, J. Phys. B **18**, L489 (1985).
[40] J. Tulkki, Phys. Rev. A **32**, 3153 (1985).
[41] M. Ya. Amusia, V. K. Ivanov, and V. A. Kupchenko, J. Phys. B **14**, L667 (1981).
[42] W. Jitschin, U. Werner, G. Materlik, and G. D. Doolen, Phys. Rev. A **35**, 5038 (1987).
[43] I. P. Grant, in *X-Ray and Inner-Shell Processes* (Ref. [15]), p. 46.
[44] K. G. Dyall and R. E. LaVilla, Phys. Rev. A **34**, 5123 (1986).
[45] V. Schmidt, Rep. Prog. Phys. **55**, 1484 (1992).
[46] U. Becker, D. Szostak, H. G. Kerkhoff, M. Kupsch, B. Langer, R. Wehlitz, A. Yagishita, and T. Hayaishi, Phys. Rev. A **39**, 3902 (1989).
[47] M. Ya. Amusia, L. V. Chernysheva, G. F. Gribakin, and K. L. Tsemekhman, J. Phys. B **23**, 393 (1990).
[48] A. Kodre, I. Arčon, M. Hribar, M. Štuhec, and F. Villain, J. Phys. (Paris) Colloq. (to be published).
[49] G. Wendin and M. Ohno, Phys. Scr. **14**, 148 (1976).